ICCPGE 2016, 1, 25 - 30

# Experimental and Theoretical Study of Laminar Boundary Layer over Flat Plate

Mohamed M. El-Mayit<sup>1,\*</sup>, Ahmed A. B. Alarabi<sup>2</sup>, Najla D. A. Alhwinat<sup>2</sup>

<sup>1</sup>Department of Mechanical Power Engineering, Minoufiya University, Shibin El-Kom, Egypt

<sup>2</sup>Department of Mechanical Engineering, College of Engineering Technology, Hoon, Libya

\*\*Corresponding Author:

#### Abstract

Air flowing past a solid surface will stick to that surface. This phenomenon caused by viscosity. This condition states that the velocity of the fluid at the solid surface equals the velocity of that surface. The result of this condition is that a boundary layer is formed in which the relative velocity varies from zero at the wall to the value of the relative velocity at some distance from the wall. The goal of the present research is to study the boundary layer characteristics over a flat plate theoretically and experimentally. The studied parameters were the mass flow rate ratio, the distance from the plate leading edge and the surface type i.e. smooth and roughness. All the experiments were carried in the fluid mechanics laboratory at College of Engineering Technology – Hoon, Libya. The results show that the boundary layer thickness over smooth surface is higher than that in the rough surface condition. The boundary layer thickness was found to be increases with the increase of both mass flow rate ratio and downstream distance (i.e. distance from the leading edge). Good agreement was obtained between experimental and theoretical results of laminar flow over the flat plate.

Keywords: Boundary layer thickness; mass flow rate ratio; smooth surface; Rough surface, Leading edge.

# 1. Introduction

A boundary layer is the thin region of flow adjacent to a surface, the layer in which the flow is influenced by the friction between the solid surface and the fluid. The boundary layer thickness denoted by the symbol  $(\delta)$ . The theory that described the flow over surfaces and bodies assuming the flow to be inviscid, incompressible and irrotational – and on the other hand there was the field of hydraulics which was a mainly experimental field concerning the behaviour of fluids in machinery like pipes. Boundary layer theory playing a major rule in aerodynamics (airplanes, rockets, projectiles), hydrodynamics (ships, submarines, torpedoes), transportation (automobiles, trucks, cycles), wind engineering (buildings, bridges, water towers), and ocean engineering (buoys, breakwaters, cables).

The properties of a turbulent boundary layer were investigated related to the drag for a two dimensional fence by K. G. Ranga et.al.[1]. The measurements were obtained at zero pressure gradient of velocity profiles along smooth, rough and transitional flat plates. A simple formula for the displacement thickness and the local shear coefficient has been predicted. This formula was modified to the universal velocity defect law for equilibrium boundary layers. P.-å. Krogstad et.al [2] carried measurements in a zero-pressure-gradient turbulent boundary layer over a mesh-screen rough wall indicate several differences, in both inner and outer regions, in comparison to a smooth-wall boundary layer. The mean velocity distribution indicates that, apart from the expected k-type roughness function shift in the inner region, the strength of



the rough-wall outer region 'wake' is larger than on a smooth wall. The Comparison between smooth and rough-wall spectra of the normal velocity fluctuation suggested that the strength of the active motion may depend on the nature of the surface. A. E. Perry et.al. [3], presented an experimental study of turbulent boundary-layer development over rough walls in both zero and adverse pressure gradients. They chose two wall roughness geometries each giving a different law of behavior on the study. One type gives a Clauses type roughness function which depends on a Reynolds number based on the shear velocity and on a length associated with the size of the roughness. The other type of roughness (typified by a smooth wall containing a pattern of narrow cavities). They indicated that the corresponding roughness function does not depend on roughness scale, but depends instead on the pipe diameter. The results obtained for both types of roughness to be correlated with a Reynolds number based on the wall shear velocity and on the distance below the crests of the elements. The Levy-Lees form of the laminar boundary layer equations was solved by F.G. Blottner [4] with several second-order accurate finite-difference schemes. The results of this investigation show that the coupled continuitymomentum form of the Crank-Nicolson scheme is second-order with one iteration at each step and requires less time than the Keller box scheme.

M. P. Schultz et.al. [5] were investigated the turbulence measurements for rough-wall boundary layers and the results then compared with smooth wall boundary layer. The rough-wall experiments were made on a three-dimensional rough surface geometrically. The experiments covered a wide Reynolds-number range (2180–27100). In this investigation, the root-mean-square roughness height was at least three orders of magnitude smaller than the boundary-layer thickness, and the Kármán number ( $\delta+$ ), typifying the ratio of the largest to the smallest turbulent scales in the flow, was as high as 10100. The results lend strong support to the concept of outer layer similarity for rough walls in which there is a large separation between the roughness length scale and the largest turbulence scales in the flow.

The structure of the flat plate incompressible smoothent is also large enough to have a very significant surface boundary layer in a low-speed water flow effect on the turbulence structure. A modified is examined by H. T. Kim et.al. [6] using hydrogen-bubble measurements and also hot-wire measure-lation was studied by W. F. Klinksiek et.al. [12]

ments with dye visualization. The results show that, the velocity profiles during bursting periods assume a shape which is qualitatively distinct from the well-known mean profiles.

A. E. Perry et.al. [7], investigated experimentally the turbulence structure in smooth and rough wall . The results for mean flow, turbulence intensity and spectral data for both smooth and rough surfaces ,were supported for the attached eddy hypothesis of Townsend (1976), the model for wall turbulence proposed by Perry & Chong (1982) and the extended version developed by Perry, Henbest & Chong (1986).

The governing equations for a laminar flow were solved by F.G. Blottner et.al.[8] in terms of an orthogonal surface coordinate system. One of the coordinate is determined by the intersection with the body surface of meridional planes which pass through an axis containing the stagnation point. The other coordinate is obtained numerically from the orthogonality condition. The momentum equations was replaced with a nonlinear finite-difference equation which is solved as an iterative solution of linear tridiagonal equations. Numerical calculations based on the compressible boundary-layer equations and an integral form of the kinetic energy of turbulence (IKET) equation were investigated for a variety of conditions by Hodge, B. K et.al.[9]. They concluded that the IKET-based extended mixing-length hypothesis more flexible than conventional mixing-length turbulence mod-

Calculation of boundary layer development using the turbulent energy equation was studied by P. Bradshaw et.al .[10]. The turbulent energy equation was converted into a differential equation by defining three empirical functions relating the turbulent intensity, diffusion and dissipation to the shear stress profile. Calculation of boundary layer development using the turbulent energy equation ,compressible flow on adiabatic walls was investigated by P. Bradshaw et.al [11]. The study was focused on the compressible flow in two-dimensional boundary layers in arbitrary pressure gradient . They pointed that, in supersonic flow, surface curvature which is large enough to induce a significant longitudinal pressure gradieffect on the turbulence structure. A modified Crank-Nicholson implicit finite difference formulation was studied by W. F. Klinksiek et.al. [12]



for two and three-dimensional turbulent boundary layers. The turbulent stresses were treated after Prandtl's early mixing length model. The specific empirical input is the Maise and McDonald mixing length model.

# 2. Experimental Work

All the experiments were carried in the fluid mechanics laboratory at College of Engineering Technology – Hoon, Libya. The experiments were carried using the air flow bench device.

# 2.1. Description of Apparatus of The Experimental

The experimental rig consists of the following main parts:

- Centrifugal fan with specifications ( Type SC 8  $\times 2$  .50 with height and width of 27.5cm , and 30cm respectively, and power supply 220/240V ).
- Air intake section which designed in such away the air flowing in a parallel streams.
- The pressure gauge fitted at the end of intake section.
- The test section where the flat plate is installed.
- Measurement tools such oil manometers, pressure gauge, and pitot tube.

Figure 2.1a shows the arrangement of the test section attached to the outlet of the contraction of the air flow bench .A flat plate is placed at mid height of the section ,with a sharpened edge facing the oncoming flow. One side of the plate is smooth and the other is rough so that by turning the plate over, results may be obtained on both types of surface. Figure 2.1b shows the photo of the test rig used in this work.

#### 2.2. Experimental Procedure

The flat firstly has to be fixed in its specified place at the required leading edge, secondly the centrifugal fan will be operated at adjustment mass flow rate starting from highest percent (  $\dot{m}/\dot{m}$ max = 1.00 ) to the lowest value (  $\dot{m}/\dot{m}$ max = 0.25 ). Each mass flaw rate has a corresponding flow velocity ( free steam velocity which denoted by the symbol U $\infty$ . At each mass flow rate the leading

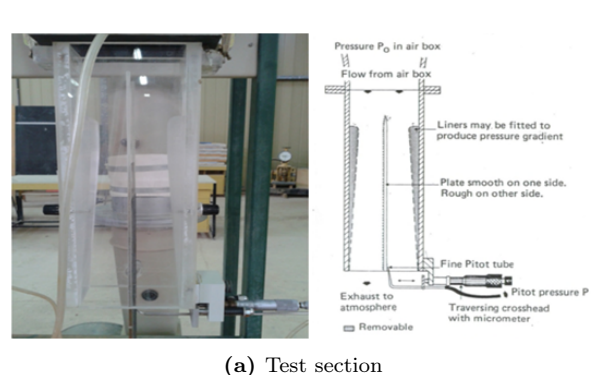
edge of the flat plate will be fixed at three different positions from the nose of the pitot tube. The leading edge distances (x) were 130 mm, 180 mm and 230 mm. The pitot tube then will be adjusted at the surface of the plate that it touches the surface of the flat plate. At the surface, the flow velocity considered to be zero. The pitot tube will be moved away from the surface in steps each 0.25 mm till reaching the free velocity zone. The difference between the total head and static head measured by a special oil manometer. For each measurement a limited time from two to three minutes has to be taken to reach the stability at the oil manometer heads. The results of all experimental work are shown in figures [4-7].

# 3. Theoretical Work

This section deals with converting the boundary layer equations in the form of partial differential equations into finite difference scheme. By using the Crank Nicolson method, the boundary layer equations were solved by using Matlab programmer. The laminar boundary layer equations for both compressible and incompressible fluid flow along the flat plate were solved theoretically. The theoretical results were compared with the experimental results for incompressible laminar boundary layer on flat plate.

#### 3.1. Finite Differences

Finite differences procedure used to solve a PDE. A finite difference procedure is presented for solving coupled sets of partial differential equations. For one dependent variable, the procedure consists of replacing a single unknown at multiple grid points with the concept of a line of node points with multiple unknowns at each node point. The process is illustrated first for a second order, linear elliptic partial differential equation and then for a coupled set of non-linear elliptic partial differential equations. The procedure could be extended to include three spatial coordinates and time, suppose that we wish to solve PDE for which u(x, y) is the dependent variable, where the square domain  $0 \le x \le 1$ ,  $0 \le y \le 1$ . A grid was established on the domain by replacing u(x, y) by  $u(i\Delta x, j\Delta y)$ . Points can be located according to values of i and j, so difference equations are usually written in terms of the general point (i, j) and its neighbors . This labeling is illustrated in Figure 2.1: Apparatus of the experimental





(b) Photo graph of used test rig

then,  $x_1 = x_2 + x_3 = x_4 + x_5 = x_4 + x_5 = x_5$ 

$$u_{i+1,j} = u(x_0 + \Delta x, y_0), \ u_{i-1,j} = u(x_0 - \Delta x, y_0)$$
  
 $u_{i,j+1} = u(x_0, y_0 + \Delta y), \ u_{i,j-1} = u(x_0, y_0 - \Delta y)$ 

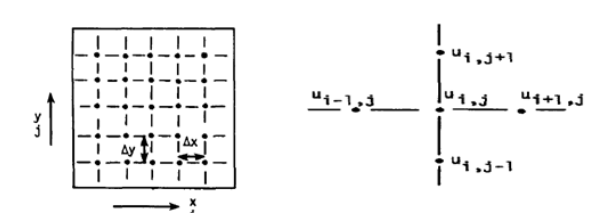


Figure 3.1: Typical finite difference grid

Most of the PDEs arising in fluid mechanics and heat transfer involve only first and second partial derivatives , and generally , we strive to represent these derivatives using values at only two or three grid points . Within these restrictions, the most frequently used first-derivative approximations on grid for which  $\Delta x = {\rm const.}$  are:

• The forward finite-difference:

$$\left(\frac{\partial u}{\partial x}\right)_{i,j} = \frac{u_{i+1,j} - u_{i,j}}{\Delta x} \tag{3.1}$$

• The backward finite-difference:

$$\left(\frac{\partial u}{\partial x}\right)_{i,j} = \frac{u_{i,j} - u_{i-1,j}}{\Delta x} \tag{3.2}$$

• The central finite-difference:

$$\left(\frac{\partial u}{\partial x}\right)_{i,j} = \frac{u_{i+1,j} - u_{i-1,j}}{2\Delta x} \tag{3.3}$$

Figure 3.1. Thus , if we think of ui , j as  $\mathbf{u}(x_0,y_0)$ ,  $\bullet$  The derivatives using values at three grid points:

$$\left(\frac{\partial u}{\partial x}\right)_{i,j} = \frac{-3u_{i,j} + 4u_{i+1,j} - u_{i+2,j}}{2\Delta x} \quad (3.4)$$

$$\left(\frac{\partial u}{\partial x}\right)_{i,j} = \frac{3u_{i,j} - 4u_{i+1,j} + u_{i+2,j}}{2\Delta x}$$
 (3.5)

The most common three-point second-derivative approximations for a uniform grid,  $\Delta x = const$ , are:

$$\left(\frac{\partial^{2} u}{\partial x^{2}}\right)_{i,j} = \frac{u_{i,j} - 2u_{i+1,j} + u_{i+2,j}}{\left(\Delta x\right)^{2}}$$
(3.6)

$$\left(\frac{\partial^2 u}{\partial x^2}\right)_{i,j} = \frac{u_{i,j} - 2u_{i-1,j} + u_{i-2,j}}{\left(\Delta x\right)^2}$$
(3.7)

$$\left(\frac{\partial^2 u}{\partial x^2}\right)_{i,j} = \frac{u_{i+1,j} - 2u_{i,j} + u_{i-2,j}}{(\Delta x)^2}$$
 (3.8)

# 3.2. Laminar Boundary Layer Equations in Finite Difference for Incompressible Flow

The assumption of incompressible laminar steady flow are ( the speed V<100 m/s or M<0.3 , where M is the Mach number, constant density and Re  $<5{\times}10^5$  ).

Momentum Equation:

$$u\frac{\partial u}{\partial x} + v\frac{\partial u}{\partial y} = u_e \frac{\partial u_e}{\partial x} + v\frac{\partial^2 u}{\partial y^2}$$
 (3.9)

$$\begin{split} & \frac{\left[\theta u_{j}^{n+1} + (1-\theta)u_{j}^{n}\right]\left(u_{j}^{n+1} - u_{j}^{n}\right)}{\Delta x} + \\ & \frac{\left[\theta v_{j}^{n+1}\left(u_{j+1}^{n+1} - u_{j-1}^{n+1}\right) + (1-\theta)v_{j}^{n}\right]u_{j+1}^{n} - u_{j-1}^{n}}{2\Delta y} \\ & = \frac{\left[\theta u_{e}^{n+1} + (1-\theta)u_{e}^{n}\right]\left(u_{e}^{n+1} - u_{e}^{n}\right)}{\Delta x} \\ & + \frac{v}{\left(\Delta y\right)^{2}} \left[\theta\left(u_{j+1}^{n+1} - 2u_{j}^{n+1} + u_{j-1}^{n+1}\right) \\ & + (1-\theta)\left(u_{j+1}^{n} - 2u_{j}^{n} + u_{j-1}^{n}\right)\right] \\ & (3.10) \end{split}$$

For flat plate  $\left(\frac{\partial u_e}{\partial x} = 0\right)$ 

Where  $\theta$  is weighting factor if:

- = 0 (Method is explicit).
- = 1/2 (Crank-Nicolson implicit).
- = 1 (Fully implicit).

### **Continuity Equation:**

$$\frac{\partial u}{\partial x} + \frac{\partial v}{\partial y} = 0 (3.11)$$

$$\frac{v_j^{n+1} - v_{j-1}^{n+1}}{\Delta y} + \frac{u_j^{n+1} - u_j^n + u_{j-1}^{n+1} - u_{j-1}^n}{2\Delta x} = 0$$
(3.12)

#### Momentum Equation:

$$u\frac{\partial u}{\partial x} + v\frac{\partial u}{\partial y} = u_e \frac{\partial u_e}{\partial x} v \frac{\partial^2 u}{\partial y^2}$$
 (3.13)

$$\frac{\left[\theta u_{j}^{n}+(1-\theta)u_{j}^{n}\right]\left(u_{j}^{n+1}-u_{j}^{n}\right)}{\Delta x}+\\ \frac{\left[\theta v_{j}^{n+1}\left(u_{j+1}^{n+1}-u_{j-1}^{n+1}\right)+(1-\theta)v_{j}^{n}\right]}{2\Delta y}\\ *\left(u_{j+1}^{n}-u_{j-1}^{n}\right)=\\ \frac{\left[\theta u_{e}^{n}+(1-\theta)u_{e}^{n}\right]\left(u_{e}^{n+1}-u_{e}^{n}\right)}{\Delta x}$$

$$(3.14)$$

$$B_j^n u_{j-1}^{n+1} + D_j^n u_j^{n+1} + A_j^n u_{j+1}^{n+1} = C_j^n$$
 (3.15)

Where,

$$D_j^n = \frac{u_j^n}{\Delta x} + \frac{2\nu\theta}{(\Delta y)^2} \tag{3.16}$$

$$B_j^n = -\frac{\theta v_j^n}{2\Delta y} - \frac{\upsilon \theta}{\left(\Delta y\right)^2} \tag{3.17}$$

$$C_{j}^{n} = \frac{\left(u_{j}^{n}\right)^{2}}{\Delta x} - \frac{\left(1 - \theta\right) v_{j}^{n} u_{j+1}^{n} - u_{j-1}^{n}}{2\Delta y} + \frac{v\left(1 - \theta\right) \left(u_{j+1}^{n} - 2u_{j}^{n} + u_{j-1}^{n}\right)}{\left(\Delta y\right)^{2}}$$
(3.18)

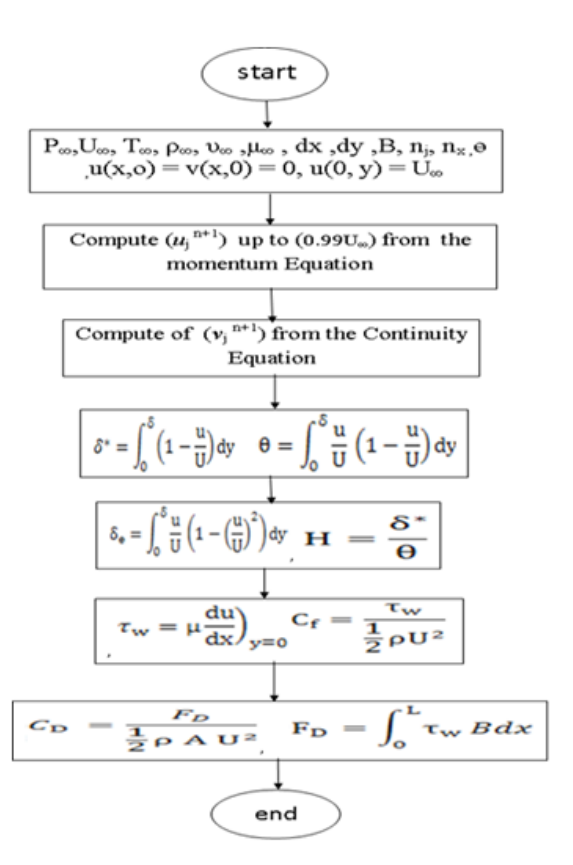


Figure 3.2: Flow chart for solving laminar incompressible boundary layer on flat plate



#### Continuity Equation:

$$\frac{v_j^{n+1} - v_{j-1}^{n+1}}{\Delta y} + \frac{u_j^{n+1} - u_j^n + u_{j-1}^{n+1} - u_{j-1}^n}{2\Delta x} = 0$$
(3.19)

$$CC_j^n = \left(\frac{u_j^{n+1} - u_j^n + u_{j-1}^{n+1} - u_{j-1}^n}{2\Delta x}\right) \Delta y \quad (3.20)$$

$$v_j^{n+1} = v_{j-1}^{n+1} - CC_j^n (3.21)$$

The data have been supplied to the computer program using Mat lap technique and the results for laminar steady incompressible flow over the flat plate as shown in the flow chart on Figure 3.2, where the theoretical results are shown in Figure 4.5 [a,b].

#### 4. Results and Discussion

Figure 4.1 (a, b, c and d) show the velocity profile over a rough flat plate. In all tested conditions it found that the boundary layer profile has a parabolic shape. The fluid particles at the flat plate surface have zero velocity and they act as a retardant to reduce velocity of adjacent particles in the vertical direction. The velocity of the fluid increases as it released from surface drag till reaches maximum value at the boundary layer edge where the flow velocity is equal about 99% of the free stream flow velocity (i.e., u=0.99U.). It is concluded that, at any location of the rough flat plate, the boundary layer thickness increases with increasing the mass flow rate. From these figures it can be observed that along the downstream distance, the magnitude of the velocity decreased due to friction effect. From these figures it can be noticed that more elongation in the velocity profile curve means higher boundary layer thickness. To show the effect of mass flow rate more accurate, the variation of flow velocity along the flat plate surface are shown in Figure 4.1d.

Figure 4.2 (a ,b,c and d) shows the velocity profile over a smooth flat plate. It can be seen that the velocity profile has the same trend as that for the rough surface, this means that the surface roughness has no effect on the velocity profile shape.

By comparing the boundary thickness it can be noticed that the boundary layer thickness in the condition of rough surface is higher than that in the case of smooth surface, this occurred mainly due to friction at flow surface. Also at the same vertical distance it can be seen that the velocity magnitude in the smooth surface is higher than that in rough surface condition due to low friction degree in the smooth surface condition.

The effect of surface roughness is shown Figure 4.3(a, b, c and d) at different mass flow rates. It can be seen that the smooth surface velocity profile is more wider than that of rough surface profile. The Figure shows that the rough boundary layer thickness is bigger than that of smooth surface boundary layer thickness and this mainly occurred due to the drag force caused by the surface. By comparing both rough and smooth surface, it can be observed that a considerable effect occurred due to surface roughness degree.

Figure 4.4 (a and b) shows the effect leading edge distance on the boundary layer thickness. It can be seen that the boundary layer thickness increases with increasing the leading edge distance, i.e. the boundary layer grows as the traveling distance is increased and the curves tend to have a greater tangent as velocity increases. Figure 4.5 (a and b) shows the theoretical results of laminar boundary layer thickness characteristics at different operating parameters. Figure 4.5a shows the effect leading edge distance on the boundary layer thickness. The computer program obtained the same trend of the boundary layer thickness as that obtained experimentally. Logically there are some deviation between the theoretical and experimental results which will be discussed in comparisons graphs.

Figure 4.6 (a, b, c, and d) shows the comparisons of theoretical and experimental results of laminar boundary layer thickness at different operating parameters. It can be seen that the comparison was carried at different working parameters such as free stream flow velocities, and different leading edge distances. Figure 4.5 proves that good agreement was obtained between experimental and theoretical results. The average of error values is less than 4.5%. The comparison shows that the theoretical model has good approximation in the range of the laminar flow, more precisely in smooth surface application.

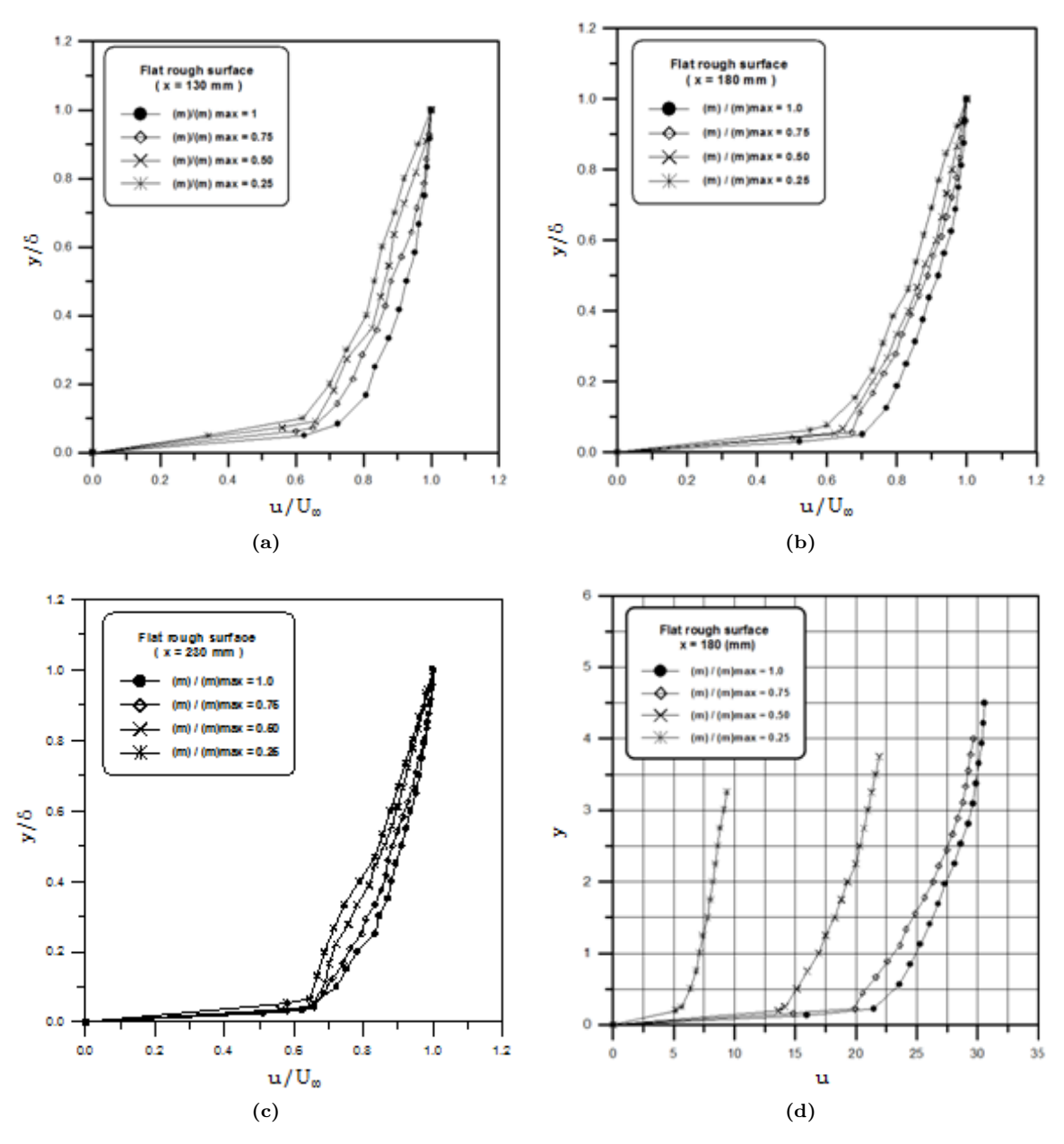


Figure 4.1: Velocity profile over flat rough plate at different mass flow rates

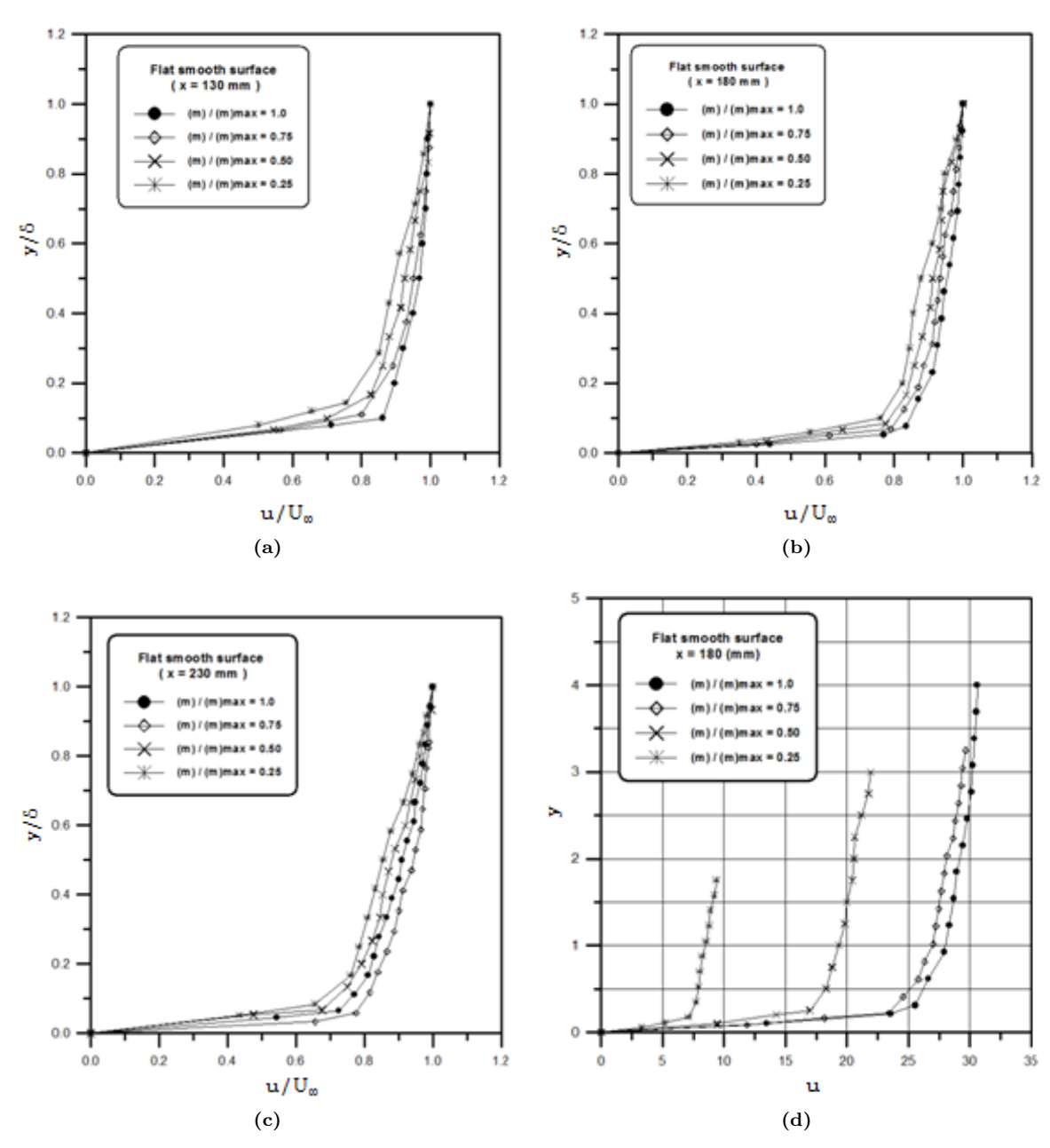
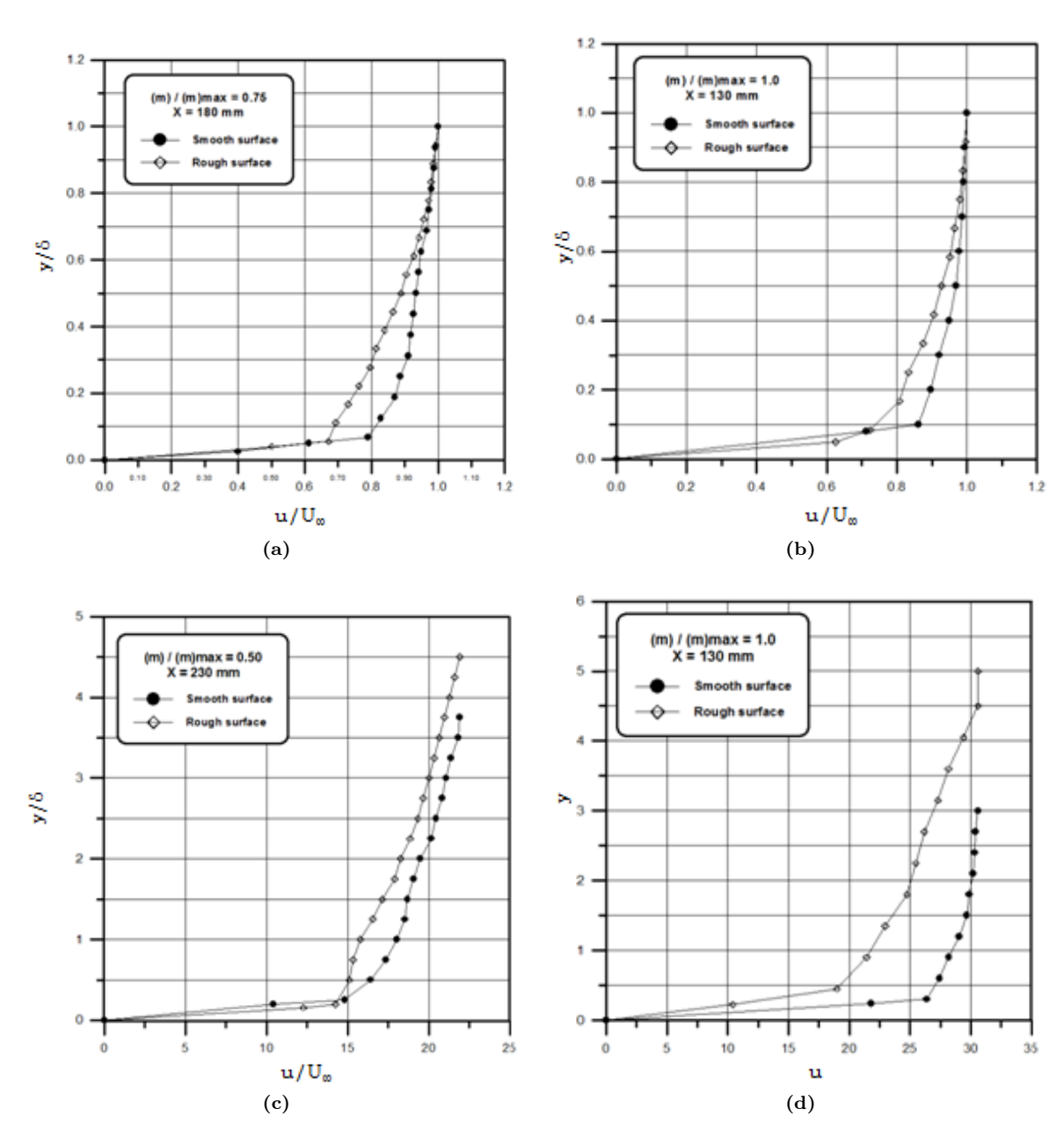


Figure 4.2: Velocity profile over flat smooth plate at different mass flow rates



 $\textbf{Figure 4.3:} \ \, \textbf{Effect surface roughness on velocity profile over flat plate at different mass flow rates}$ 

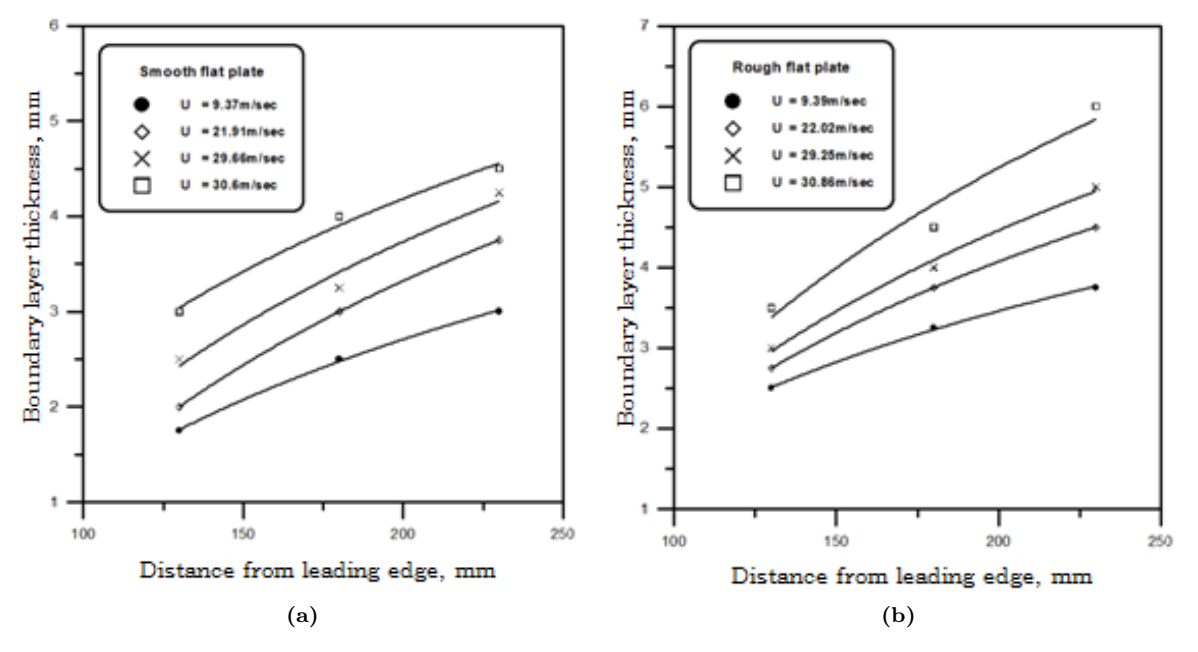


Figure 4.4: Effect of leading edge distance on boundary layer thickness

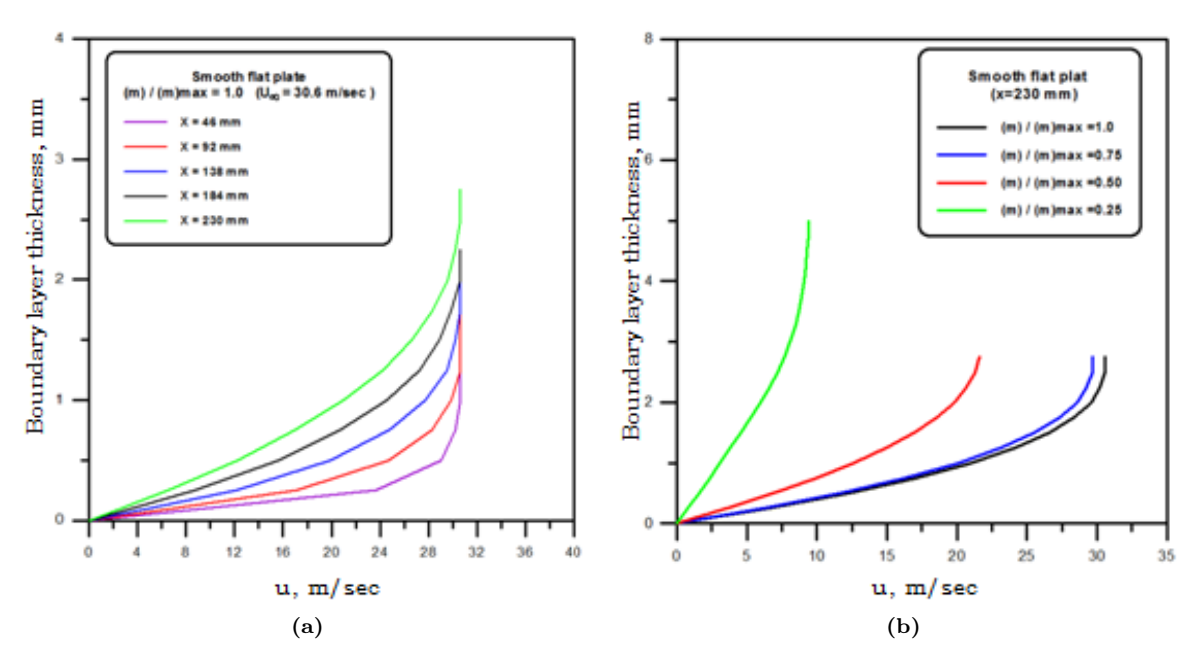


Figure 4.5: Theoretical results of boundary layer thickness at different operating parameters

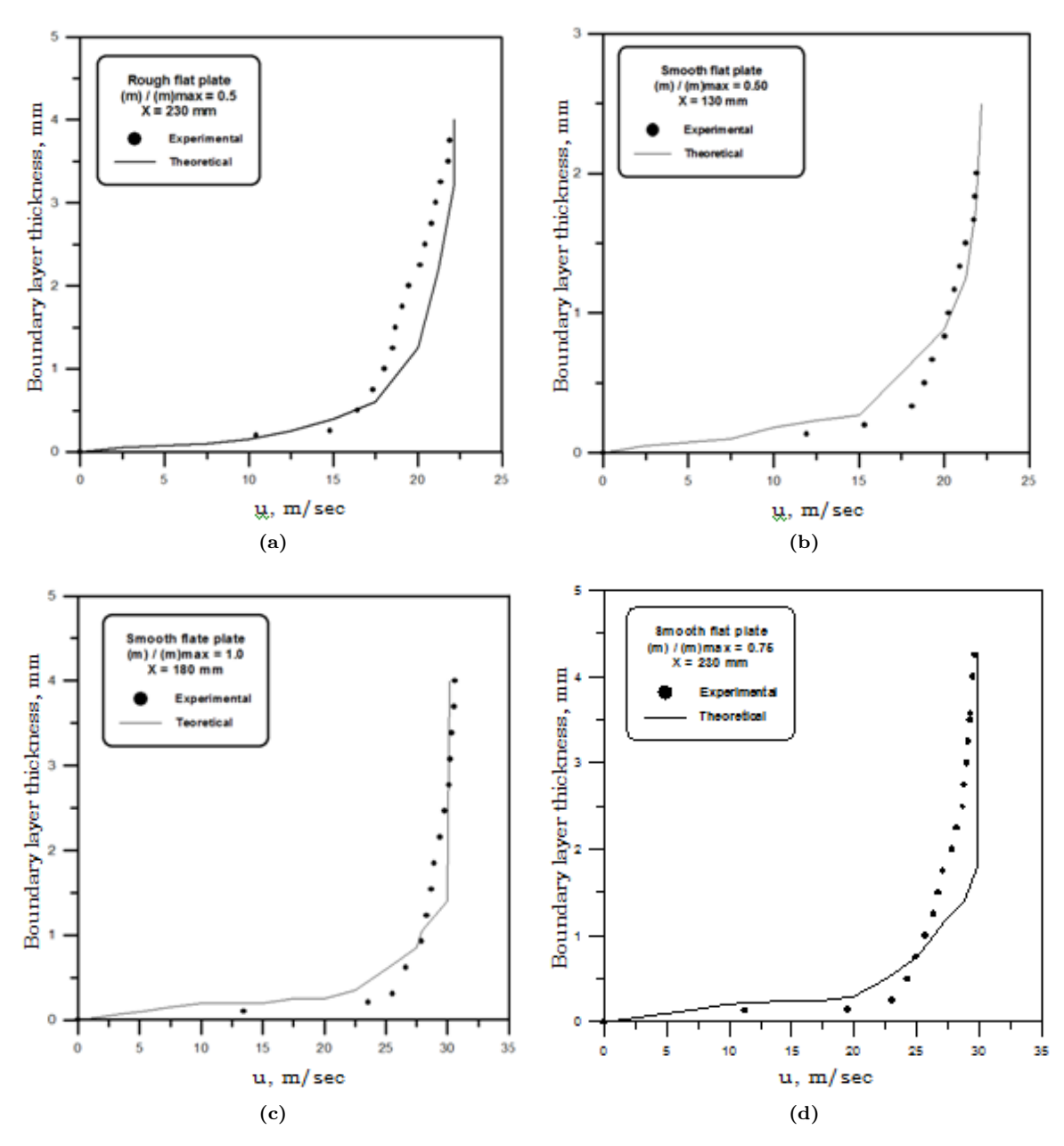


Figure 4.6: Comparisons of theoretical and experimental results of boundary layer thickness at different operating parameters

#### 5. Conclusion

The following points were concluded:

- At all tested conditions, the boundary layer thickness increases with increasing the mass flow rate i.e. ( free stream flow velocity ).
- The boundary layer thickness increases with increasing the leading edge distance.
- The rough surface boundary layer thickness is higher than smooth boundary layer thickness.
- The surface type i.e. smooth or rough has tha major effect on the boundary layer thickness.

# 6. Acknowledgment

The authors gratefully acknowledge the technical support given by the department of mechanical engineering at College of Engineering Technology, Hoon

# References

- [1] K. G. Ranga Raju, J. Loeser, and E. J. Plate . Velocity profiles and fence drag for a turbulent boundary layer along smooth and rough flat plates. Institute Wasserbau III, University of Karlsruhe, Germany, April, 11, 2006
- [2] P. Krogstad , R. A. Antonia, and L. W. B. Browne. Comparison between roughand smooth-wall turbulent boundary layers. Journal of Fluid Mechanics, 1992, 245, 599 -617.
- [3] A. E. Perry, W. H. Schofield and P. N. Joubert. Rough wall turbulent boundary layers.
   Journal of Fluid Mechanics, June 1969, 383

   413, Published online 2006.
- [4] F.G. Blottner. Investigation of some finitedifference techniques for solving the boundary layer equations. Proceedings of the Second International Conference on Numerical Methods in Fluid Dynamics, 2005, 8, 144-150.
- [5] M. P. Schultz and K. A. Flack. The roughwall turbulent boundary layer from the hydraulically smooth to the fully rough regime. Journal of Fluid Mechanics, 2007, 580, 381–405.

- [6] H. T. Kim a1p1, S. J. Kline a1 and W. C. Reynolds a1" The production of turbulence near a smooth wall in a turbulent boundary layer. Journal of Fluid Mechanics, 1971, 50, 133 – 160, Published online: 2006.
- [7] A. E. Perry, K. L. Lim and S. M. Henbest. An experimental study of the turbulence structure in smooth- and rough-wall boundary layers. Journal of Fluid Mechanics, 1987, 177, 534 – 535, Published online: 2006.
- [8] F.G. Blottner and Molly A. Ellis. Finitedifference solution of the incompressible three-dimensional boundary layer equations for a blunt body. Computers & Fluids Journals, 1973, 1, 119-233.
- [9] J. Adams, JR.B, and Hodge. The calculation of compressible transitional, turbulent, and relaminarizational boundary layers over smooth and rough surfaces using an extended mixing-length hypothesis. 10th Fluid and Plasmadynamics Conference, 1977, 77, page 682.
- [10] P. Bradshaw, D. H. Ferriss and N. P. Atwell. Calculation of boundary-layer development using the turbulent energy equation. Journal of Fluid Mechanics, 1967, 28, 593 – 616, Published online 2006.
- [11] P. Bradshaw and D. H. Ferriss. Calculation of boundary-layer development using the turbulent energy equation: compressible flow on adiabatic walls. Journal of Fluid Mechanics, 1971, 46, 83 110, Published online 2006.
- [12] W.F.Klinksiek and F. J. Pierce"A Finite Difference Solution of the Two and Three-Dimensional Incompressible Turbulent Boundary layer Equations. Journal of Fluid Mechanics, 1973, 95, 445-458, Published online 2010.